The above experiments and SOM provide an atomic-level perspective on the formation of warm dense matter. The observations demonstrate that warm dense gold is formed in a purely thermal process. Previously observed quasi–steady state signatures in the optical response cannot be assigned to instantaneous, nonthermal formation of a liquid-like state. The difference in the rate of substantial superheating and lattice disordering, at the predicted electronic temperatures for increased lattice stability, supports a photo-induced bond hardening mechanism and the concept of a T_e-dependent melting temperature. The increased lattice stability will also increase the barrier to nucleation as the electron distribution and nuclear configurations are strongly coupled. Full-scale ab initio molecular dynamics calculations are now needed to understand this phenomenon to which the experiment provides rigorous benchmarks for comparison.

References and Notes

1. B. J. Siwick, J. R. Dwyer, R. E. Jordan, R. J. D. Miller, *Science* **302**, 1382 (2003).
2. A. Rousse *et al.*, *Nature* **410**, 65 (2001).
3. A. M. Lindenberg *et al.*, *Science* **308**, 392 (2005).
4. V. Recoules, J. Clérouin, G. Zérah, P. M. Anglade, S. Mazevet, *Phys. Rev. Lett.* **96**, 055503 (2006).
5. F. Bottin, G. Zérah, *Phys. Rev. B* **75**, 174114 (2007).
6. M. Kandyla, T. Shih, E. Mazur, *Phys. Rev. B* **75**, 214107 (2007).
7. R. Biswas, V. Ambegaokar, *Phys. Rev. B* **26**, 1980 (1982).
8. E. S. Zijlstra, J. Walkenhorst, M. E. Garcia, *Phys. Rev. Lett.* **101**, 135701 (2008).
9. M. Harb *et al.*, *Phys. Rev. Lett.* **100**, 155504 (2008).
10. K. Sokolowski-Tinten *et al.*, *Nature* **422**, 287 (2003).
11. D. M. Fritz *et al.*, *Science* **315**, 633 (2007).
12. Z. Lin, L. V. Zhigilei, *Phys. Rev. B* **73**, 184113 (2006).
13. C. Guo, A. J. Taylor, *Phys. Rev. B* **62**, R11921 (2000).
14. K. Widmann *et al.*, *Phys. Rev. Lett.* **92**, 125002 (2004).
15. T. Ao *et al.*, *Phys. Rev. Lett.* **96**, 055001 (2006).
16. S. Mazevet, J. Clérouin, V. Recoules, P. M. Anglade, G. Zérah, *Phys. Rev. Lett.* **95**, 085002 (2005).
17. Y. Ping *et al.*, *Phys. Rev. Lett.* **96**, 255003 (2006).
18. J. R. Dwyer *et al.*, *Philos. Trans. R. Soc. London. Ser. A* **364**, 741 (2006).
19. C.-Y. Ruan, Y. Murooka, R. K. Raman, R. A. Murdick, *Nano Lett.* **7**, 1290 (2007).
20. A. Plech, V. Kotaidis, S. Gresillon, C. Dahmen, G. von Plessen, *Phys. Rev. B* **70**, 195423 (2004).
21. C. T. Hebeisen *et al.*, *Opt. Express* **16**, 3334 (2008).
22. J. Hohlfeld *et al.*, *Chem. Phys.* **251**, 237 (2000).
23. G. Radi, *Acta Crystallogr. A* **26**, 41 (1970).
24. Z. Lin, L. V. Zhigilei, V. Celli, *Phys. Rev. B* **77**, 075133 (2008).
25. B. Rethfeld, K. Sokolowski-Tinten, D. von der Linde, S. I. Anisimov, *Phys. Rev. B* **65**, 092103 (2002).
26. B. J. Siwick, J. R. Dwyer, R. E. Jordan, R. J. D. Miller, *Chem. Phys.* **299**, 285 (2004).
27. A. M. Lindenberg *et al.*, *Phys. Rev. Lett.* **100**, 135502 (2008).
28. D. S. Ivanov, L. V. Zhigilei, *Phys. Rev. B* **68**, 064114 (2003).
29. We thank A.-A. Dhirani and the Emerging Communications Technology Institute at the University of Toronto for the usage of their deposition chambers and L. Zhigilei, Z. Lin, and S. Mazevet for helpful discussions. We also thank A. Ng for initial discussions that led to this study. Funding was provided by the Natural Science and Engineering Research Council. R.E. thanks the Alexander von Humboldt Foundation for financial support.

Switching Off Hydrogen Peroxide Hydrogenation in the Direct Synthesis Process

Jennifer K. Edwards,[1] Benjamin Solsona,[1] Edwin Ntainjua N,[1] Albert F. Carley,[1] Andrew A. Herzing,[2,3] Christopher J. Kiely,[3] Graham J. Hutchings[1]*

Hydrogen peroxide (H_2O_2) is an important disinfectant and bleach and is currently manufactured from an indirect process involving sequential hydrogenation/oxidation of anthraquinones. However, a direct process in which H_2 and O_2 are reacted would be preferable. Unfortunately, catalysts for the direct synthesis of H_2O_2 are also effective for its subsequent decomposition, and this has limited their development. We show that acid pretreatment of a carbon support for gold-palladium alloy catalysts switches off the decomposition of H_2O_2. This treatment decreases the size of the alloy nanoparticles, and these smaller nanoparticles presumably decorate and inhibit the sites for the decomposition reaction. Hence, when used in the direct synthesis of H_2O_2, the acid-pretreated catalysts give high yields of H_2O_2 with hydrogen selectivities greater than 95%.

Hydrogen peroxide (H_2O_2) is an important commodity chemical used primarily for disinfection and bleaching (*1*) and will be used in the future for the manufacture of propylene oxide using the titanium silicalite TS-1 as a catalyst (*2*). It is currently produced by an indirect process in which H_2 and O_2 are kept apart using the sequential hydrogenation and oxidation of an anthraquinone (*2*). For economic reasons, the indirect process is carried out on a large scale

and produces concentrated H_2O_2, although most applications require very dilute solutions. Direct processes that oxidize H_2 have been investigated, and supported palladium catalysts are known to be effective (*3–5*). However, as in any redox process where a reactive intermediate is required as the final product, the key problem is stabilizing the resulting H_2O_2 so that it does not decompose and form water. Indeed, all catalysts so far identified for direct H_2O_2 synthesis are equally effective for its sequential hydrogenation or decomposition to water (*6–12*) (Scheme 1), and acid and halides must be added to ensure that some H_2O_2 is retained (*6, 9–12*).

To date, the best H_2 selectivity reported for the direct synthesis process using Pd is ~80% (*3*). We have shown (*8, 13–16*) that alloying gold with palladium markedly enhances the catalyst activity and selectivity, with a selectivity of 80%

being achieved even in the absence of halide and acid promoters (*17*). For commercial competitiveness with the indirect process, it is essential that H_2 selectivity is increased to >95%. We have now addressed this problem and show that acid pretreatment of carbon support materials can switch off the sequential hydrogenation and decomposition of H_2O_2, thereby achieving the target selectivities and producing high rates of H_2O_2 synthesis under intrinsically safe conditions.

We have previously investigated a variety of support materials for Au-Pd catalysts (*8, 13, 14, 16*) and, specifically, the selectivities for H_2 utilization under our standard reaction conditions (*18*) are carbon (80%) ~ SiO_2 (80%) > TiO_2 (70%) > Al_2O_3 (14%) (*17*). To understand these selectivity differences, we investigated the hydrogenation and decomposition of H_2O_2 over these catalysts and supports (Table 1). The oxide supports showed no activity in the absence of the metals, but the carbon support did show some reactivity, as noted previously (*15*). When the metals are added, all show appreciable activity for these nonselective reactions with the order of activity being broadly in line with the observed H_2 selectivities in the synthesis reaction. Because these catalysts are prepared by wet impregnation of an acidic solution of the metal salts onto the support (*18*), we investigated the effect of an initial acid pretreatment step in which the support
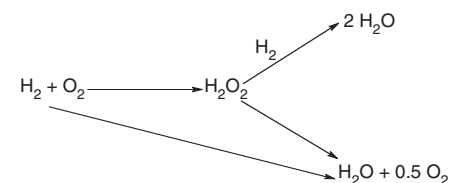
[1]School of Chemistry, Cardiff University, Main Building, Park Place, Cardiff CF10 3AT, UK. [2]National Institute of Standards and Technology, Surface and Microanalysis Science Division, 100 Bureau Drive, Mailstop 8371, Gaithersburg, MD 20899–8371, USA. [3]Center for Advanced Materials and Nanotechnology, Lehigh University, 5 East Packer Avenue, Bethlehem, PA 18015–3195, USA.

*To whom correspondence should be addressed. E-mail: hutch@cardiff.ac.uk

Scheme 1.

was treated with 2% aqueous HNO_3 and dried before addition of the metals ([18]). For the Au-Pd catalysts on oxide supports, this step led to a decrease in combined hydrogenation and decomposition, but for the carbon support, the Au-Pd catalysts showed no such activity when reacting a 4 weight percent (wt %) H_2O_2 solution (Table 1).

To investigate this effect, we examined the stability of higher concentration solutions of H_2O_2 using the carbon-supported materials. Solutions of H_2O_2 were stirred with high pressure H_2 (5% H_2/CO_2, 3 MPa) in the presence of the support or the catalyst (10 mg) for 30 min at 2°C (i.e., standard reaction conditions without the addition of O_2); representative data are shown in Fig. 1. Pd and Au-Pd catalysts on untreated carbon, as well as the bare support itself, react in a similar manner and give sequential hydrogenation. These results show that the support plays a crucial role in the performance of catalysts for the direct reaction because it controls the manner in which the active components are dispersed, as well as providing the sites on which H_2O_2 hydrogenation-decomposition, and hence product loss, occurs. However, the acid-pretreated carbon support shows some reduction in H_2O_2 hydrogenation activity relative to the nontreated material, but when it is loaded with Pd the rate of hydrogenation of H_2O_2 becomes identical to that of the corresponding nontreated Pd/C catalyst, showing that the nonselective hydrogenation sites have been restored (Fig. 1A). In stark contrast, the acid-pretreated Au-Pd alloy catalyst shows no substantial activity for the sequential hydrogenation of H_2O_2, up to 14 wt % H_2O_2, and only at a concentration of 17.5 wt % does some sequential hydrogenation begin to occur.

We then investigated the carbon-supported Au-Pd catalysts at 2°C using nonexplosive dilute H_2/O_2 mixtures [($H_2 < 4$ volume percent (vol %)] with CO_2 as a diluent and using methanol/water as a solvent; under these conditions, we observed a marked increase in the yield of H_2O_2 and the selectivity of H_2 utilization (Table 2, experiments 1 to 3). No enhancement was observed for similarly pretreated Pd-only catalysts (Table 2, experiments 4 to 6), whereas a slight positive effect is still observed for pretreated Au catalysts (Table 2, experiments 7 to 9). An enhancement was always observed with the Au-Pd alloy catalysts when the acid pretreatment was conducted before metal addition (Table 2, experiments 1 to 3). Nitric and acetic acids were the most effective acids tested to date (Table 2, experiments 9 to 12), whereas base pretreatment with ammonium hydroxide invariably led to a decrease in yield (Table 2, experiment 13). Treatment with water alone, or ammonium, sodium, or potassium nitrates had no effect (Table 2, experiments 2, 14 to 16), confirming that it is the exposure to acid that is important. The materials prepared using acid-pretreated supports combined with a calcination at 400°C were found to give catalysts that could be reused several times (Fig. 1B) without any loss of performance. For each use, the acid-pretreated catalyst gave an initial rate of 640 mol

H_2O_2 $kg_{cat}^{-1}.h^{-1}$ determined at 2 min reaction time, and 160 mol H_2O_2 $kg_{cat}^{-1}.h^{-1}$ determined at 30 min reaction time, with 40% hydrogen conversion. The addition of nitric acid to the reaction mixture before H_2O_2 synthesis—which is an established procedure for stabilizing H_2O_2 ([1], [2], [10]–[12]) because H_2O_2 decomposition is known to be a base catalyzed process—also led to an enhancement in the yield of H_2O_2, but the effect was not sustained upon subsequent catalyst reuse (Fig. 1B). Treatment of any of the supports after metal deposition did not enhance catalyst performance, and addition of nitric or hydrochloric acid during the metal impregnation step did not lead to any enhancement (Table 2, experiments 17,18); indeed, the addition of hydrochloric acid was deleterious. These results demonstrate the importance of the precise manner in which the acid pretreatment is carried out. However, neither the acid concentration nor the duration of

the acid pretreatment are critical; the effect can be observed even when quite dilute acid solutions (2 vol %) are used.

Interestingly, both the untreated and the acid-pretreated Au catalyst also show no activity for sequential hydrogenation (Fig. 1A); unfortunately, both these catalysts also show remarkably little activity for H_2O_2 synthesis (Table 2, experiments 7 to 9). However, these results do show that the adsorption of Au onto the surface of the carbon support blocks the sites responsible for loss of H_2O_2 because the catalyst has no activity for the decomposition reaction. Hence, we consider that it is the interaction of Au with the pretreated C support that is crucial for observing this new effect of switching off H_2O_2 hydrogenation/decomposition. The switch-off phenomenon was also observed after the acid-pretreated Au-Pd/C catalysts had been used for the direct synthesis reaction, and, indeed, this effect was sustained after several

Table 1. Effect of acid pretreatment of the support on the hydrogenation and decomposition of H_2O_2.

	Support only				Au-Pd catalyst*			
	Untreated		Pretreated†		Untreated		Pretreated†	
Support	Hydrog‡	Decomp§	Hydrog‡	Decomp§	Hydrog‡	Decomp§	Hydrog‡	Decomp§
Al_2O_3	0	0	0	0	24	3	16	8
TiO_2	0	0	0	0	12	6	13	4
SiO_2	0	0	0	0	15	8	12	1
Carbon	4	1	3	1	5	2	0	0

*Catalysts contain 2.5 wt % Au–2.5 wt % Pd co-impregnated onto the support (wt % = mass fraction).   †Treated with 2% HNO_3 in aqueous solution (volume fraction = 2% HNO_3).   ‡H_2O_2 hydrogenation conditions: catalyst (10 mg), 2.9 MPa H_2 (volume fraction 5%)/CO_2, 2°C, 0.5 hours, methanol/water as solvent, stirring rate 1200 rpm (126 rad/s).   §H_2O_2 decomposition conditions: catalyst (10 mg), air, atmospheric pressure, 2°C, 0.5 hours, methanol/water as solvent, stirring rate 1200 rpm.

Table 2. Activity and selectivity of pretreated and untreated carbon-supported catalysts for H_2O_2 synthesis at 2°C. All catalysts calcined in air 400°C for 3 hours. Reaction conditions: 10 mg catalyst using carbon as support, 2.9 MPa H_2 (5% volume fraction)/CO_2 1.1 MPa O_2 (25% volume fraction)/CO_2, 2°C, 0.5 hours, methanol/water as solvent, pretreated as indicated for 30 min.

Experiment number	Catalyst*	Pretreatment†	H_2O_2 selectivity (%)	Productivity (mol kg_{cat}^{-1} h^{-1})
1	2.5% Au–2.5% Pd/carbon	None	80	110
2	2.5% Au–2.5% Pd/carbon	Water	80	112
3	2.5% Au–2.5% Pd/carbon	2% HNO_3	>98	160
4	5% Pd/carbon	None	42	50
5	5% Pd/carbon	Water	42	50
6	5% Pd/carbon	2% HNO_3	42	52
7	5% Au/carbon	None	nd‡	0.4
8	5% Au/carbon	Water	nd‡	0.4
9	5% Au/carbon	2% HNO_3	nd‡	0.5
10	2.5% Au–2.5% Pd/carbon	2% CH_3COOH	>98	175
11	2.5% Au–2.5% Pd/carbon	2% H_3PO_4	30	120
12	2.5% Au–2.5% Pd/carbon	2% HCl	15	130
13	2.5% Au–2.5% Pd/carbon	2% NH_4OH	24	70
14	2.5% Au–2.5% Pd/carbon	2% NH_4NO_3	80	100
15	2.5% Au–2.5% Pd/carbon	2% KNO_3	80	120
16	2.5% Au–2.5% Pd/carbon	2% $NaNO_3$	80	122
17	2.5% Au–2.5% Pd/carbon	HCl§‖	5	20
18	2.5% Au–2.5% Pd/carbon	HNO_3§‖	35	98

*Metal loadings denoted as mass fractions.   †Acid concentration expressed in terms of volume fraction.   ‡Not determined due to yields being very low.   §Added to slurry during catalyst preparation.   ‖Concentration 1 kmol/m^3 in aqueous solution.

uses. Hence, the catalysts can be used multiple times without loss of activity for the direct H_2O_2 formation reaction or gaining activity for H_2O_2 hydrogenation/decomposition.

We carried out a direct synthesis reaction with the pretreated AuPd/C catalyst in the presence of H_2O_2 (4.3 wt %), and after 30 min of reaction additional H_2O_2 is produced (0.1 wt %), whereas with the untreated catalyst only decomposition/ hydrogenation is observed (*18*). The opposing reactivity of this pair of catalysts directly shows that the acid pretreatment has switched off the sequential hydrogenation of H_2O_2 for the Au-Pd catalyst, thus leading to the observed enhanced activities and selectivities. In our synthesis experiments, we used a stirred autoclave and can only synthesize relatively dilute H_2O_2 solutions. However, the acid-pretreated Au-Pd/C catalysts could be used in a set of sequential experiments in which the gases were repeatedly replenished at 30-min intervals (Fig. 1C). Acid-pretreated Au-Pd catalysts steadily increased the H_2O_2 concentration, whereas untreated Pd and Au-Pd catalysts exhibited markedly inferior performance because of enhanced H_2O_2 hydrogenation/decomposition.

Bulk and surface analysis of the acid pretreated supported catalysts revealed no marked distinguishing characteristics (figs. S1 to S3) (*18*), but our previous scanning transmission electron microscopy (STEM) annular dark field (ADF) analysis of the untreated Au-Pd/C sample revealed a trimodal particle size distribution (*19*). The smallest particles fell in the range of 2 to 5 nm, intermediate size particles were ~10 to 50 nm in size, and occasional particles were observed exceeding 70 nm. X-ray energy dispersive spectroscopy (STEM-XEDS) spectrum images also showed that the composition of the metal nanoparticles varied with size in a systematic manner (*19*), such that the smallest particles tended to be Pd-rich whereas the largest particles were highly Au-rich.

However, as shown in the STEM-XEDS spectrum image data presented in Fig. 2, A to F, and fig. S4 (*18*), no surface segregation of Pd or Au was detected in either the untreated or acid pretreated catalysts, and this was confirmed by x-ray photoemission spectroscopy (XPS) (figs. S2 and S3) (*18*). Instead, all of the particles were homogeneous Au-Pd alloys, in contrast to the core-shell structure observed previously in similar Au-Pd particles on oxide supports. Finally, the STEM-XEDS data indicates that the acid pretreatment does not appear to alter the trend in the particle-size/composition dependence, and, thus, the switching off of H_2O_2 hydrogenation/decomposition and enhancement in activity observed with acid pretreatment is not caused by the specific morphology changes of the Au-Pd alloy particles.

A major difference between the acid-treated and untreated Au-Pd/C samples was found in the alloy particle size distribution (see the histogram in Fig. 2G). Acid pretreatment of the support improved nanoparticle nucleation and favored the formation of a greater number fraction of the smallest (Pd-rich alloy) particles at the expense of the intermediate (similar Au-Pd content) and large (Au-rich) particles, which is consistent with the increased surface Au content determined from XPS (figs. S2 and S3) (*18*). The acid-pretreated Au-Pd/C sample exhibited only the small (2 to 5 nm) and intermediate (10 to 50 nm) Au-Pd homogeneous alloy particles of similar composition to their counterparts observed in the untreated sample. Furthermore, no Au-Pd particles >50 nm were found in the acid-pretreated catalyst, whereas very large Au-rich particles were readily observed on the untreated carbon support. Thus, the beneficial effect of acid pretreatment is to enhance the gold dispersion in the bimetallic alloy particles by generating smaller Au-Pd nanoparticles, and these presumably decorate sites on the support that are otherwise active for the hydrogenation/decomposition of H_2O_2. The increase in activity for the direct synthesis of H_2O_2 is therefore due to the formation of smaller active alloy nanoparticles, and the enhancement in selectivity toward H_2O_2 is caused by these small particles switching off the active sites for H_2O_2 decomposition. The observation that small nanoparticles are required for high activity is consistent with recent observations for Au and Pd catalysts (*20–22*).

We find similar effects for pure Au/C catalysts where the acid pretreatment decreases the average Au particle size (Fig. 2H). Interestingly, no such effect is observed for the dispersion of pure Pd/C (Fig. 2I), which is consistent with the concomitant lack of enhancement in the catalytic
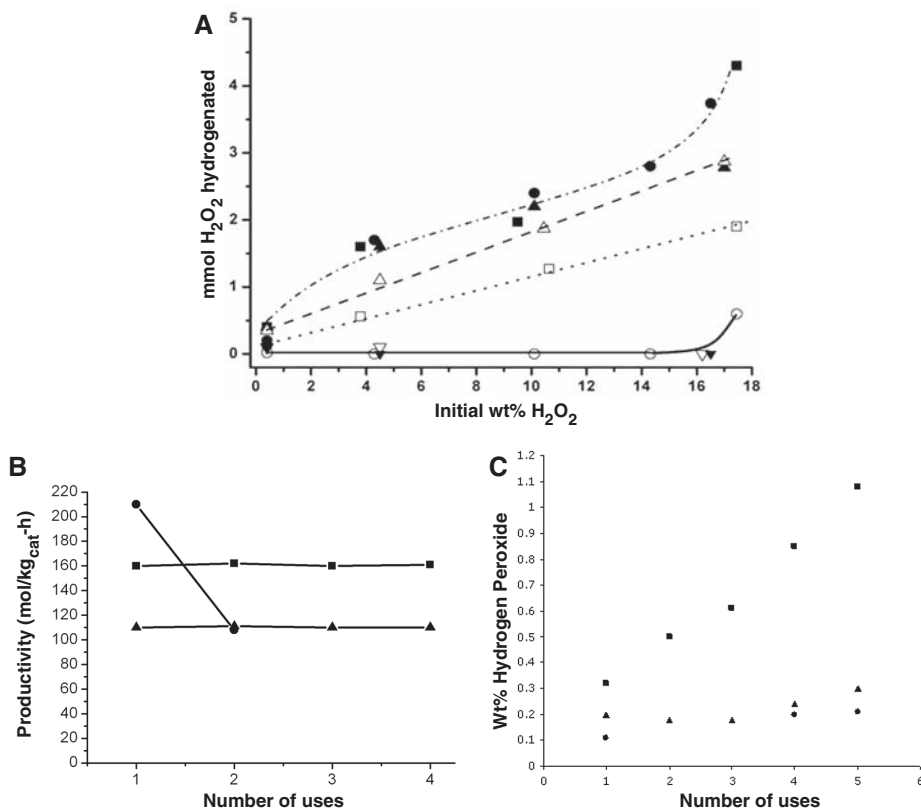

Fig. 1. (**A**) Performance of acid-pretreated carbon-supported catalysts compared with nontreated catalysts for the hydrogenation of H_2O_2. Dashed-dotted line: filled squares, untreated 2.5% Au–2.5% Pd/C; filled circles, untreated carbon support. Dashed line: filled triangles, untreated 5% Pd/C; open triangles, pretreated 5% Pd/C. Dotted line: open squares, pretreated support. Solid line: open circles, pretreated 2.5% Au–2.5% Pd/C; inverted open triangles, pretreated 5% Au /C; inverted filled triangles, untreated 5% Au /C. Reactions were carried out with H_2O_2 in solvent [methanol (5.6 g) and water (2.9 g)] at 2°C with 1200 rpm, stirring for 30 min under 420 psig (2.90×10^6 Pa) 5% H_2/CO_2. The data show that for the pretreated Au-Pd and Au catalysts the hydrogenation and decomposition of H_2O_2 is switched off, whereas extensive hydrogenation/decomposition is observed with nontreated AuPd and Pd catalysts; results are shown for the extent of hydrogenation/decomposition (wt % = mass fraction). (**B**) Performance of acid-pretreated catalysts compared with nontreated catalysts for the synthesis of H_2O_2. The untreated (triangles) and 2% HNO_3 treated (squares) catalysts are stable over four uses, with the latter showing a higher activity. The addition of 2% HNO_3 in the autoclave with the untreated catalyst (circles) shows a higher initial activity that is lost on subsequent reuse (it remains at the same level as the untreated catalyst in subsequent reuses). (**C**) The effect of sequential experiments using gas top-up on hydrogen peroxide concentration. The acid-treated Au-Pd/carbon (squares) catalyst shows increasing hydrogen peroxide concentration as reactant gases are refreshed (*18*). In contrast, the untreated Au-Pd/carbon (triangles) catalyst and 5% Pd/carbon (circles) catalyst show no increase in hydrogen peroxide concentration as the gases are refreshed, due to enhanced hydrogen peroxide hydrogenation/decomposition for the nontreated catalysts.

performance due to acid pretreatment (Table 2, experiments 4 to 6). Apparently, to observe this particle size redistribution, Pd has to be alloyed with Au. Hence, we conclude that the acid pretreatment of the carbon support, by itself, leads to a partial decrease in the active sites for nonselective hydrogenation, which gives rise to a subsequent improvement in the dispersion of the Au-Pd alloy particles and leads to a complete switching off of the sites for sequential hydrogenation. This effect is probably achieved by Au altering the physical or electronic structure of Pd sufficiently to inhibit

its hydrogenation ability. This inhibition is analogous to the observation by Goodman and co-workers (23) for Au-Pd model catalysts for the synthesis of vinyl chloride monomer (VCM), where Au promoted the reaction through a slight alteration of the atomic spacing of Pd, which did not affect VCM synthesis but did inhibit its decomposition.

The results above are based on small-scale experiments in a stirred autoclave for short reaction periods (30 min). In a further set of experiments designed to examine the stability of these catalysts, we stirred the pretreated catalyst (100 mg) in the

reaction medium (5.6 g MeOH and 2.9 g H_2O) in the presence of the reaction gases (5% H_2/CO_2 and 25% O_2/CO_2 mixed to give a H_2/O_2 mol ratio = 1:2, 3.7 MPa) at 2°C for 98 hours. We then recovered the catalyst that had been aged in this way and carried out the synthesis of H_2O_2 under standard reaction conditions and found that the reactivity and selectivity were identical to that of a fresh catalyst. In addition, the key effect had been retained because the decomposition of H_2O_2 remained switched off in the aged catalyst. We also note from high-angle ADF (HAADF)
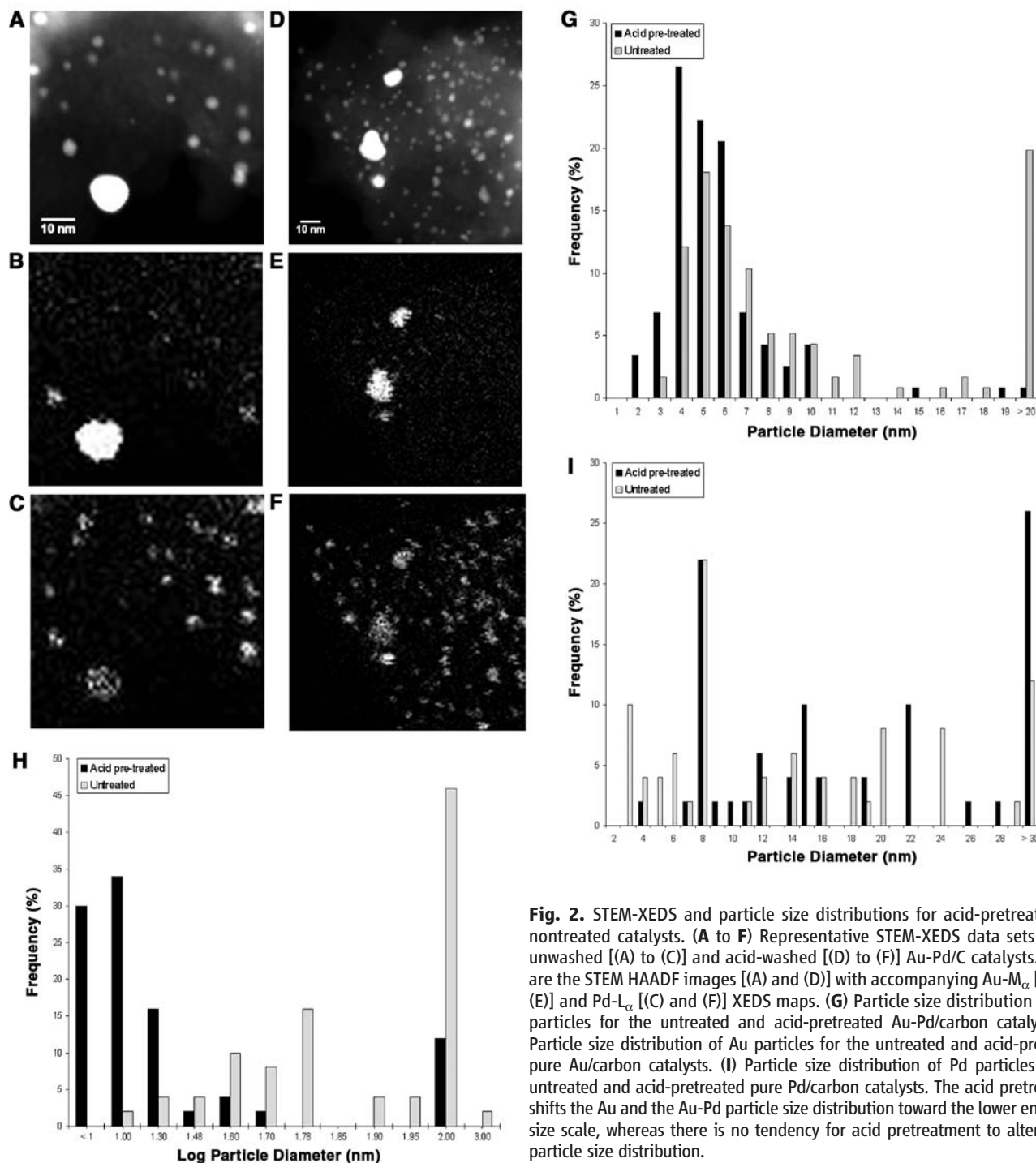
Fig. 2. STEM-XEDS and particle size distributions for acid-pretreated and nontreated catalysts. (**A** to **F**) Representative STEM-XEDS data sets for the unwashed [(A) to (C)] and acid-washed [(D) to (F)] Au-Pd/C catalysts. Shown are the STEM HAADF images [(A) and (D)] with accompanying Au-M_α [(B) and (E)] and Pd-L_α [(C) and (F)] XEDS maps. (**G**) Particle size distribution of alloy particles for the untreated and acid-pretreated Au-Pd/carbon catalysts. (**H**) Particle size distribution of Au particles for the untreated and acid-pretreated pure Au/carbon catalysts. (**I**) Particle size distribution of Pd particles for the untreated and acid-pretreated pure Pd/carbon catalysts. The acid pretreatment shifts the Au and the Au-Pd particle size distribution toward the lower end of the size scale, whereas there is no tendency for acid pretreatment to alter the Pd particle size distribution.

imaging (fig. S5) (*18*) that intermediate and small particles are retained in the catalyst after the 98-hour aging treatment. Hence, the beneficial effect of the acid pretreatment is not short lived. We consider that with appropriate development and reaction engineering (i.e., scaling up using continuous flow reactors with pelleted or extruded catalyst formulations), our discovery, made using powdered catalysts in a small-scale batch autoclave reactor, can underpin the generation of H_2O_2 at the 3 to 8% concentration levels required in most chemical and medical applications

One benefit of the direct process (*24*) is that it will permit local synthesis on a small scale as and when required, thereby ensuring that H_2O_2 no longer needs to be stored or transported, both of which are potentially hazardous, as demonstrated by a recent road tanker explosion in the United Kingdom (*25*). In particular, the process lends itself to small-scale generation of H_2O_2, which could be of great value for the production of medical antiseptics where the H_2 would be generated from water by electrolysis.

References and Notes

1. H. T. Hess *et al.*, Eds., *Kirk-Othmer Encyclopedia of Chemical Engineering* (Wiley, New York, 1995).
2. J. Van Weynbergh, J. P. Schoebrechts, J. C. Colery, U.S. Patent 5447706, (1992).
3. J. H. Lunsford, *J. Catal.* **216**, 455 (2003).
4. D. P. Dissanayake, J. H. Lunsford, *J. Catal.* **206**, 173 (2002).
5. D. P. Dissanayake, J. H. Lunsford, *J. Catal.* **214**, 113 (2003).
6. V. R. Choudhary *et al.*, *Chem. Commun. (Camb.)* **2004**, 2054 (2004).
7. P. Landon *et al.*, *Phys. Chem. Chem. Phys.* **5**, 1917 (2003).
8. J. K. Edwards *et al.*, *J. Mater. Chem.* **15**, 4595 (2005).
9. M. J. Maraschino, U.S. Patent 5169618 (1992).
10. V. R. Choudhary, C. Samanta, *J. Catal.* **238**, 28 (2006).
11. V. R. Choudhary, P. Jana, *J. Catal.* **246**, 434 (2007).
12. V. R. Choudhary *et al.*, *Appl. Catal.* **317**, 234 (2007).
13. J. K. Edwards *et al.*, *Catal. Today* **122**, 397 (2007).
14. B. E. Solsona *et al.*, *Chem. Mater.* **18**, 2689 (2006).
15. J. K. Edwards *et al.*, *Faraday Discuss.* **138**, 225 (2008).
16. J. K. Edwards *et al.*, *J. Catal.* **236**, 69 (2005).
17. J. K. Edwards *et al.*, *Green Chem.* **10**, 388 (2008).
18. Materials and methods are available as supporting material on *Science* Online.
19. A. A. Herzing *et al.*, *Faraday Discuss.* **138**, 337 (2008).
20. Q. Liu *et al.*, *Angew. Chem. Int. Ed.* **47**, 6221 (2008).
21. M. Turner *et al.*, *Nature* **454**, 981 (2008).
22. A. A. Herzing *et al.*, *Science* **321**, 1331 (2008).
23. M. Chen *et al.*, *Science* **310**, 291 (2005).
24. *The Chemical Engineer* **766**, 16 (2005).
25. BBC News, 30 August 2005; http://news.bbc.co.uk/1/hi/england/london/4197500.stm
26. Supported by the Engineering and Physical Sciences Research Council of the United Kingdom and Johnson Matthey PLC (project ATHENA) and the European Union (project AURICAT, HPRN-CT-2002-00174). C.J.K. and A.A.H. are funded by: NSF DMR-0079996, NSF DMR-0304738, and NSF-DMR-0320906. A.A.H. thanks the NRC for support through the postdoctoral associate program. We thank A. Roberts and C. Blomfield (Kratos Analytical) for assistance with XPS measurements, and P. Collier, P. Ellis, and P. Johnston (Johnson Matthey) for discussions on analysis, provision of ICP analysis data, and design of the sequential experiments.

Strong Release of Methane on Mars in Northern Summer 2003

Michael J. Mumma,[1]* Geronimo L. Villanueva,[2,3] Robert E. Novak,[4] Tilak Hewagama,[3,5] Boncho P. Bonev,[2,3] Michael A. DiSanti,[3] Avi M. Mandell,[3] Michael D. Smith[3]

Living systems produce more than 90% of Earth's atmospheric methane; the balance is of geochemical origin. On Mars, methane could be a signature of either origin. Using high-dispersion infrared spectrometers at three ground-based telescopes, we measured methane and water vapor simultaneously on Mars over several longitude intervals in northern early and late summer in 2003 and near the vernal equinox in 2006. When present, methane occurred in extended plumes, and the maxima of latitudinal profiles imply that the methane was released from discrete regions. In northern midsummer, the principal plume contained ~19,000 metric tons of methane, and the estimated source strength ($\geq$0.6 kilogram per second) was comparable to that of the massive hydrocarbon seep at Coal Oil Point in Santa Barbara, California.

The atmosphere of Mars is strongly oxidized, composed primarily of carbon dioxide (CO_2, 95.3%), along with minor nitrogen (N_2, 2.7%), carbon monoxide (CO, 0.07%), oxygen (O_2, 0.13%), water vapor (H_2O, 0 to 300 parts per million), and radiogenic argon (1.6%); other species and reduced gases such as methane (CH_4) are rare. CH_4 production by atmospheric chemistry is negligible, and its lifetime against removal by photochemistry is estimated to be several hundred years (*1–3*) or shorter if strong oxidants such as peroxides are present in the surface or on airborne dust grains (*4*). Thus, the presence of substantial amounts of CH_4 would require its recent release from subsurface reservoirs; the ultimate origin of this CH_4 is uncertain, but it could be either abiotic or biotic (*2, 5, 6*).

Before 2003, all searches for CH_4 were negative (*7–9*). Since then, three groups have reported detections of CH_4 (*10–18*); see (*19–24*) for discussion. Spectral data from the Mars Express mission contain five unidentified spectral features between 3000 and 3030 cm^{-1}, one of which coincides with the expected position of the CH_4 Q branch (*15, 18, 25*). The data span all seasons and extend over several years, but low S/N ratios require averaging the spectra over two of the three key dimensions (longitude, latitude, and time). Other searches featured low spatial coverage (*16*) or sparse seasonal coverage (*16, 17*), and the results (CH_4 mixing ratios) are best interpreted as upper limits.

We report measurements of CH_4 in northern summer in 2003 and estimate its source strength and its (short) destruction lifetime. Our search

covered about 90% of the planet's surface and spanned 3 Mars years (MYs) (7 Earth years). Our results (*10–14*) are based on the simultaneous detection of multiple spectrally resolved lines of CH_4, and each observation is spatially resolved, allowing examination of spatial and temporal effects. Our spatial maps reveal local sources and seasonal variations.

To search for CH_4 and other gases on Mars, we used the high-dispersion infrared spectrometers at three ground-based telescopes. Here we report data from CSHELL/IRTF (Hawaii) and NIRSPEC/Keck-2 (Hawaii) [supporting online material text 1 (SOM-1)]. Each spectrometer features a long entrance slit that is held to the central meridian of Mars (Fig. 1A) while spectra are taken sequentially in time (fig. S1). Pixelated spectra were acquired simultaneously at contiguous positions along the entire slit length, for each observation, providing 35 spectra at 0.2–arc second (arc sec) intervals (~195 km at disk center) when Mars' diameter is 7 arc sec (Fig. 1A). We binned these data (in groups of three along the slit) to provide latitudinally resolved spectra, and then in time (longitude) to improve the S/N ratio (SOM-1). Here we focus on three dates in 2003 [universal time (UT) 12 January, 19 March, and 20 March] and one in 2006 (UT 26 February) (Table 1).

Our spectra exhibit strong lines of terrestrial H_2O ($2\nu_2$ band) and CH_4 (ν_3) along with weaker lines of O_3 ($3\nu_3$) seen against the continuum (Fig. 1, B and C, top). We corrected the data for telluric extinction (SOM-2). At 3.3 μm, Mars is seen mainly in reflected sunlight, so the collected spectra also contain Fraunhofer lines (SOM-3). Removing these two components from a composite spectrum exposed the residual Mars atmospheric spectrum (Fig. 1, B and C) (*26*). One line of CH_4 and three distinct lines of H_2O are seen in each panel.

CH_4 consists of three separate nuclear spin species (A, E, and F) that act as independent

[1]NASA Goddard Space Flight Center, Mailstop 690.3, Greenbelt, MD 20771, USA. [2]Department of Physics, Catholic University of America, Washington, DC 20008, USA. [3]NASA Goddard Space Flight Center, Mailstop 693, Greenbelt, MD 20771, USA. [4]Department of Physics, Iona College, New Rochelle, NY 10801, USA. [5]Department of Astronomy, University of Maryland, College Park, MD 20742–2421, USA.

*To whom correspondence should be addressed. E-mail: michael.j.mumma@nasa.gov